The Free Internet Journal for Organic Chemistry

Paper

Archive for Organic Chemistry

Arkivoc **2026**, part __, 0-0

to be inserted by editorial office

Barbituric and thiobarbituric acid derived chromophores as anticancer agents

Akshaya Kemmasaram,[a,#] Hari Chandana, [a,b,#] Pachipala Ashrutha, [a,#] Mukesh Pashupuleti,[b,c] L. Ravithej Singh,[b,d]* and Anamika Sharma[a,b,e]*

[a]Department of Natural Products and Medicinal Chemistry, CSIR-Indian Institute of Chemical Technology, Hyderabad – 500 007, India

[b]Chemical Sciences Division, Academy of Scientific and Innovative Research, Ghaziabad – 201 002, India

[c]Division of Molecular Microbiology and Immunology, CSIR-Central Drug Research Institute, Sitapur Road, Sector 10, Janakipuram Extension, Lucknow, 226031, Uttar Pradesh, India

[d]Fluoro-Agrochemicals Division, CSIR-Indian Institute of Chemical Technology, Hyderabad – 500 007, India

[e]Peptide Sciences Laboratory, School of Physics and Chemistry, University of KwaZulu-Natal, Westville Campus, Durban 4000, South Africa

Email: lrsingh.iict@csir.res.in; anamika.aug14@gmail.com

[#]These authors contributed equally

Received mm-dd-yyyy **Accepted** mm-dd-yyyy **Published on line** mm-dd-yyyy

Dates to be inserted by editorial office

Abstract

A series of barbiturate/thiobarbiturate derivatives (**1-20**) were synthesized and evaluated for antimicrobial and anticancer activities. Three compounds were structurally confirmed by single-crystal X-ray analysis. While none showed antimicrobial activity, compounds **11-20** exhibited notable anticancer effects. Among them, compounds **15**, **16**, and **18** demonstrated promising activity against the MCF-7 cell line compared to amphotericin B, likely due to their planar molecular structures.

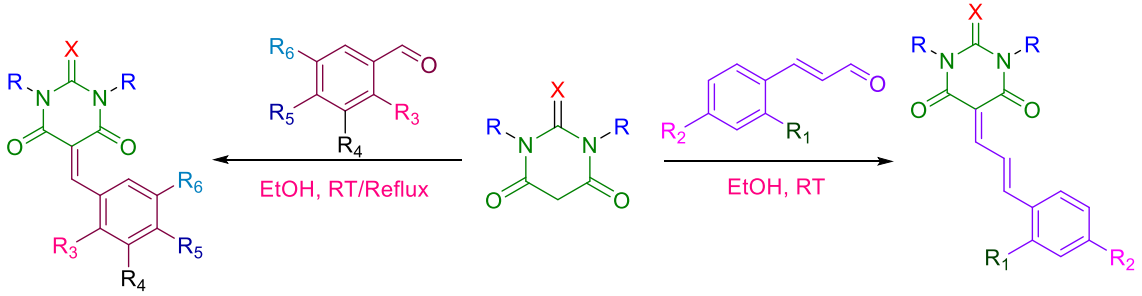

Keywords: Barbituric acid, thiobarbituric acid, antimicrobial, anticancer activity

Introduction

The continuous rise in cancer incidence and the emergence of drug resistance necessitate the development of new therapeutic agents with improved efficacy and multifunctional properties.[1, 2] In recent years, small-molecule chromophores have attracted growing attention in anticancer research, not only as imaging probes but also as biologically active agents capable of interacting with key cellular targets.[3, 4]

Among various chromophoric scaffolds, barbituric acid and thiobarbituric acid derivatives occupy a unique position due to their pronounced electron-accepting character, structural simplicity, and synthetic versatility.[5] These heterocycles readily participate in conjugated donor-acceptor systems. They have further demonstrated a wide range of biological activities, including antimicrobial, antiviral, antioxidant, and notably, anticancer properties.[6-12] Structural features such as multiple carbonyl (or thiocarbonyl) groups, activated methylene units, and hydrogen-bonding capability enable these molecules to interact efficiently with biological macromolecules, including enzymes and nucleic acids.[13] The replacement of oxygen by sulphur in thiobarbituric acid further modulates lipophilicity, polarizability, and redox behaviour, often leading to enhanced biological potency.[11]

Recent studies have shown that barbituric/thiobarbituric acid-based conjugated systems can induce cancer cell apoptosis, inhibit cell proliferation, and disrupt mitochondrial function.[6] When incorporated into extended π-systems, these scaffolds frequently display dual functionality, acting simultaneously as fluorescent probes and cytotoxic agents.[14] Such “theranostic” behaviour is particularly attractive for cancer research, as it enables both therapeutic intervention and optical tracking.

Despite these advances, systematic studies correlating molecular structure, solid-state organization, photophysical behaviour, and anticancer activity of barbituric and thiobarbituric acid-derived chromophores remain limited. In particular, the role of intermolecular interactions and crystal packing in modulating fluorescence and biological performance has received comparatively little attention.[11, 13]

In this context, we report the design and synthesis of a new series of barbituric and thiobarbituric acid-derived chromophores and their comprehensive characterization. The compounds were evaluated for their anticancer activity, and representative derivatives were further investigated by single-crystal X-ray diffraction to elucidate their molecular conformations.

Results and Discussion

Chemistry

All the derivatives were synthesized *via* Knoevenagel condensation in which the starting materials BA and TBA are reacted with different substituted aldehydes/cinnamaldehydes using ethanol as solvent (**Scheme 1**). The addition of ethanol resulted in the color change. The reaction mixture was stirred at room temperature. The formation of precipitate was observed within 10 minutes of reaction time. The formation of the product was monitored by thin layer chromatography (TLC). Once the starting materials were consumed the solvent was removed using rotary evaporator under pressure to obtain pure product in good to moderate yields. In case of **1**, the reaction mixture containing *N,N’*-dimethyl barbituric acid and 4-bromobenzaldehyde was refluxed for overnight for complete consumption of starting materials. Solvent was then removed to obtain pure product. All the synthesized derivatives were characterized by using ^{1}H NMR, ^{13}C NMR, and HRMS.

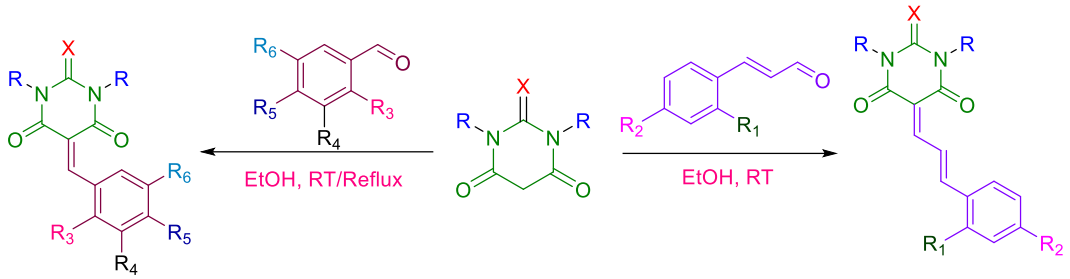

	X	R	R_3	R_4	R_5	R_6
1	O	CH_3	H	H	Br	H
2	O	CH_3	H	H	C_2H_5	H
3	O	CH_3	H	H	OCH_3	H
4	S	C_2H_5	H	H	OCH_3	H
5	S	C_2H_5	H	OCH_3	OH	OCH_3
6	O	CH_3	OCH_3	H	OCH_3	OCH_3
7	S	C_2H_5	OCH_3	H	OCH_3	OCH_3
8	O	CH_3	H	OCH_3	OCH_3	OCH_3
9	S	C_2H_5	H	OC_2H_5	OH	H
10	S	C_2H_5	H	OCH_3	OCH_3	H

	X	R	R_1	R_2
11	O	CH_3	H	H
12	S	C_2H_5	H	H
13	O	CH_3	OCH_3	H
14	S	C_2H_5	OCH_3	H
15	O	CH_3	NO_2	H
16	S	C_2H_5	NO_2	H
17	O	CH_3	H	OCH_3
18	S	C_2H_5	H	OCH_3
19	O	CH_3	H	NO_2
20	S	C_2H_5	H	NO_2

Scheme 1. Synthetic Scheme for the preparation of BA/TBA Analogues.

Crystal Structure

Compound **1** crystallizes in the triclinic system with the centrosymmetric space group P-1 and two molecules per unit cell (Z = 2). The asymmetric unit contains one independent molecule. The unit-cell parameters a = 7.9285(3) Å, b = 8.0210(4) Å, c = 11.7158(6) Å; α = 88.7261(16)°, β = 74.8280(14)°, γ = 63.1085(13)° reflect a highly distorted triclinic lattice, typical of molecules capable of multiple weak intermolecular interactions. The molecular geometry is well resolved, confirming the expected connectivity of the barbituric/thiobarbituric acid-derived scaffold. In the solid state, the molecules are stabilized through a network of weak intermolecular interactions, primarily C–H···O contacts involving the carbonyl oxygen atoms of the heterocyclic core, which contribute to the stabilization of the crystal packing. These interactions lead to the formation of one-dimensional chains, which further assemble into a three-dimensional supramolecular architecture through π–π stacking and halogen-assisted contacts involving the bromine substituent. Such interactions are likely to contribute to the observed solid-state stability and may influence the compound's photophysical behaviour.

Compound **2** crystallizes in the monoclinic crystal system with the non-centrosymmetric space group $P2_1$, containing two formula units per unit cell (Z = 2). The unit-cell dimensions a = 9.1839(9) Å, b = 5.9593(6) Å, c = 12.8027(13) Å; α = γ = 90°, β = 101.613(3)° indicate a relatively compact packing arrangement. The absence of an inversion centre suggests that the molecule adopts a chiral or conformationally biased arrangement in the solid state, which is noteworthy in the context of optical and fluorescence properties. The molecular conformation is stabilized by intramolecular interactions, while the crystal packing is influenced by weak intermolecular C–H···O contacts involving the carbonyl oxygen atoms, contributing to the formation of helical chains along the b-axis. These chains are further reinforced by van der Waals interactions, resulting in a robust three-dimensional packing motif. The non-centrosymmetric nature of this crystal may be particularly relevant for its fluorescence behaviour and potential nonlinear optical responses, complementing its biological activity profile.

Compound **8** crystallizes in the triclinic system with the space group P-1, with four molecules per unit cell (Z = 4), corresponding to two independent molecules in the asymmetric unit. The unit-cell parameters a = 9.5938(4) Å, b = 12.5580(6) Å, c = 14.3048(7) Å; α = 105.6969(16)°, β = 101.3802(17)°, γ = 98.8776(15)° reflect a significantly distorted lattice, indicative of complex intermolecular interactions.

The two independent molecules adopt slightly different conformations, highlighting a degree of conformational flexibility within the crystal. Extensive intermolecular hydrogen bonding involving multiple carbonyl and heteroatom functionalities leads to the formation of a dense supramolecular network. These interactions generate layered assemblies, which stack through additional weak contacts to stabilize the crystal packing. The presence of multiple hydrogen-bond donors and acceptors, combined with conformational variability, suggests that this compound possesses a rich solid-state interaction landscape, which may correlate with its enhanced biological activity and fluorescence response.

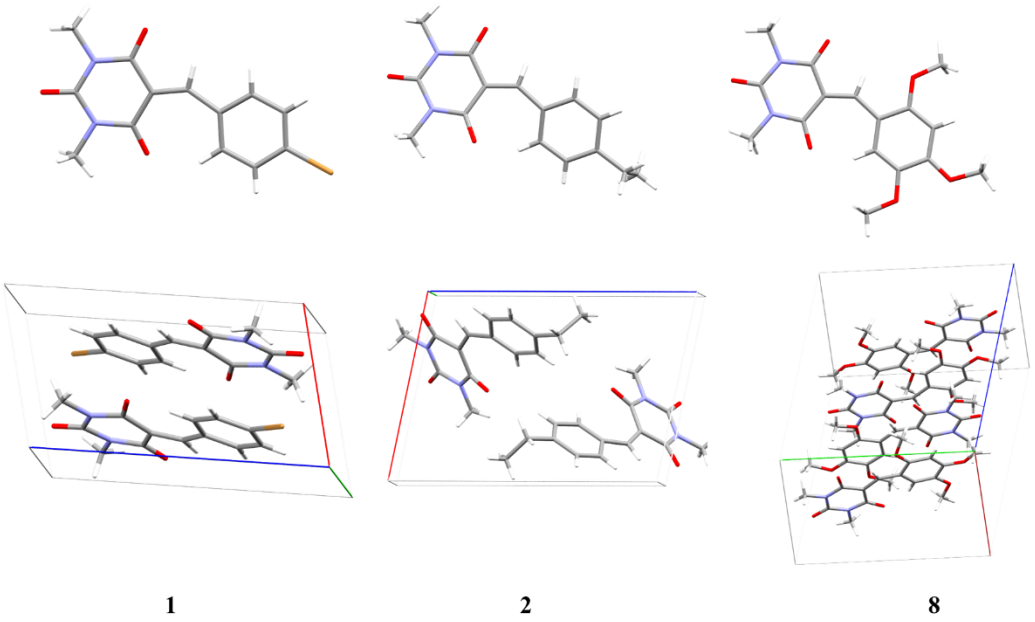

Figure 1. Ortep diagram and crystal packing in compound **1**, **2** and **8**.

Biology

All the compounds (**1-20**) were evaluated for antimicrobial and anticancer activities. The compounds were evaluated for antimicrobial activity against gram-negative bacteria [*Acinetobacter baumannii* ATCC (1605), *Klebsiella pneumoniae* ATCC (27736), *Escherichia coli* ATCC (25922), *Pseudomonas aeruginosa* ATCC (27853)], and gram-positive bacteria [*Staphylococcus aureus* ATCC (25923)]. Meropenem, ciprofloxacin, vancomycin and tigecycline were used as reference standards. None of the derivatives showed bio efficacy against the tested strains towards antimicrobial activity (*See Supporting Information, Figure S21*).

The compounds (**11-20**) were also evaluated for MTT assay against MCF-7 cell line (**Table 2**). Amphotericin-B and Meropenem were used as standard. It is evident that these derivatives displayed potent activity against MCF-7 cell line when compared with Amphotericin-B. Compounds **15**, **16** and **18** bearing nitro and methoxy substituents appeared to be the best ones among the tested series. Compounds bearing nitro at the ortho position are the most active ones compared to the ones when present at the para position. Substitution from "O" to "S" also impacted the efficacy. In case of compound **17** and **18**, bearing methoxy substitution at the para position, the later one seems to have profound effect on the bioactivity.

Table 2. IC_{50} (µg/mL) of the compounds (**1-20**) in gram-negative and gram-positive bacteria, and MCF-7 cell line, as measured using the MTT Assay

Compound Number	***AB* ATCC (1605)**	***KP* ATCC (27736)**	***EC* ATCC (25922)**	***PA* ATCC (27853)**	***SA* ATCC (25923)**	**MCF-7**

1	>50	>50	>50	>50	>50	NA
2	>50	>50	>50	>50	>50	NA
3	>50	>50	>50	>50	>50	NA
4	>50	>50	>50	>50	>50	NA
5	>50	>50	>50	>50	>50	NA
6	>50	>50	>50	>50	>50	NA
7	>50	>50	>50	>50	>50	NA
8	>50	>50	>50	>50	>50	NA
9	>50	>50	>50	>50	>50	NA
10	>50	>50	>50	>50	>50	NA
11	>50	>50	>50	>50	>50	35.0
12	>50	>50	>50	>50	>50	47.0
13	>50	>50	>50	>50	>50	32.9
14	>50	>50	>50	>50	>50	31.5
15	>50	>50	>50	>50	>50	28.5
16	>50	>50	>50	>50	>50	26.5
17	>50	>50	>50	>50	>50	45.4
18	>50	>50	>50	>50	>50	24.7
19	>50	>50	>50	>50	>50	36.4
20	>50	>50	>50	>50	>50	34.9
Meropenem	12.5	0.39	0.39	0.39	0.39	14.0
ciprofloxacin	25	0.39	0.39	0.39	0.39	-
Vancomycin	50	>50	>50	>50	0.78	-
Tigecycline	12.5	6.25	1.56	6.25	6.25	-
Amphotericin-B	-	-	-	-	-	34.8

AB: Acinetobacter baumannii; KP: Klebsiella pneumoniae; EC: Escherichia coli; PA: Pseudomonas aeruginosa; SA: Staphylococcus aureus

Conclusions

In summary, a series of compounds based on barbiturate/thiobarbiturate has been synthesized and evaluated for antimicrobial and anticancer activity. Out of all the 20 derivatives (**1-20**), three compounds crystallized as single X-ray crystal. Unfortunately, none of the compounds displayed antimicrobial activity. However, the series from **11-20** displayed satisfactory anticancer activity. Among the synthesized compounds, **15**, **16**, and **18** emerged as the most active derivatives, exhibiting IC_{50} values of 28.5, 26.5, and 24.7 µM,

respectively. The reason can also be attributed to the fact that these compounds show planer structure, a property exploited to design molecules possessing anticancer activity. These results highlight the importance of both the nature of the barbiturate core and the substituent pattern on the aromatic ring in modulating anticancer activity.

Preliminary structure-activity relationship (SAR) analysis suggests that electron-withdrawing and electron-donating substituents on the aromatic ring play a key role in determining biological activity. In particular, **15** and **16**, bearing ortho-nitro substitution, displayed enhanced cytotoxic activity, indicating that strong electron-withdrawing groups may promote favourable interactions with biological targets. Moreover, the comparison between compounds **15** (barbiturate) and **16** (thiobarbiturate) suggests that replacement of the carbonyl oxygen with sulphur can slightly improve activity, possibly due to increased lipophilicity or altered electronic properties that enhance cellular interactions. Additionally, **18**, containing a para-methoxy substituent on a thiobarbiturate scaffold, showed the lowest IC_{50} value in the series, suggesting that electron-donating groups capable of enhancing conjugation may also contribute positively to anticancer activity. Although these findings highlight the potential of barbiturate/thiobarbiturate scaffolds as anticancer agents, further structural optimization is required to improve potency and to extend activity across a broader range of cancer cell lines.

Experimental Section

General. All the chemicals were purchased from Sigma-Aldrich (Sigma-Aldrich, Germany). The solvents used were of analytical and HPLC reagent grade. Magnetic resonance spectra (^{1}H and ^{13}C) were recorded with Bruker, and chemical shift values are reported in δ units (ppm) using TMS as internal standard. Follow-up of the reactions and checks of the purity of the compound were done by TLC on silica-gel-protected aluminium sheets 60 F254 (Merck), and the spots were detected by exposure to UV light at λ = 254 nm. Analytical HPLC was performed on a Shimadzu system using a Phenomenex C18 column (3µm, 4.6×50 mm) by dissolving the sample in CH_3CN only. LabSolutions software was used for data processing. Buffer A: 0.1% TFA in H_2O, buffer B: 0.1% TFA in CH_3CN were used in HPLC. High resolution mass spectrometry (HRMS) was performed using a Bruker ESI-QTOF mass spectrometer in positive-ion mode.

Procedure for preparation of compound 1. *N,N'*-Dimethylbarbituric acid (1.1 eq.) and 4-bromobenzaldehyde (0.7 mmol, 1.0 eq.) were dissolved in ethanol and kept for reflux at 78 °C. Reaction was monitored by TLC. The reaction was stirred overnight for complete consumption of starting materials. After which the solvent was removed *via* rotary evaporation under reduced pressure and kept under high vacuum to afford the pure product.

5-(4-Bromobenzylidene)-1,3-dimethylpyrimidine-2,4,6(1*H*,3*H*,5*H*)-trione (1). Yield = 99%; **State** = Solid; **Colour** = Creamy; **^{1}H NMR** (500 MHz, $CDCl_3$): *δ* 3.37 (s, 3H, CH_3), 3.42 (s, 3H, CH_3), 7.60 (d, *J* = 8.6 Hz, 2H, ArH), 7.94 (d, *J* = 8.5 Hz, 2H, ArH), 8.47 (s, 1H, CH) ppm; **^{13}C NMR** (75 MHz, $CDCl_3$): *δ* 28.5, 29.2, 118.0, 128.0, 131.4, 131.6, 134.8, 151.1, 157.6, 160.3, 162.3 ppm; **HRMS** (APCI) m/z: Molecular formula: $C_{13}H_{11}BrN_2O_3$, calcd for $[M+H]^+$ 323.0031; Found 323.0029, ppm error 1.03.

General procedure for preparation of 1, 3-dimethyl barbituric acid and 1, 3-diethyl-2-thiobarbituric acid derivatives (2-20)

N,N' Disubstituted barbituric/thiobarbituric acid (0.6/0.5 mmol, 1.0 equiv.) and corresponding aldehyde (1.0 equiv.) were dissolved in ethanol, and the reaction was stirred at room temperature. Product formation was monitored by thin layer chromatography (TLC). After the complete consumption of starting material, the

precipitate was filtered and the residue was washed with ethanol. The residue was dried to afford the pure product.

5-(4-Ethylbenzylidene)-1,3-dimethylpyrimidine-2,4,6(1*H*,3*H*,5*H*)-trione (2)

Yield = 60%; **State** = Solid; **Colour** = Light Yellow; **^{1}H NMR** (400 MHz, $CDCl_3$): δ 1.27 (t, *J* = 7.6 Hz, 3H, CH_3), 2.73 (q, *J* = 7.6 Hz, 2H, CH_2), 3.38 (s, 3H, CH_3), 3.42 (s, 3H, CH_3), 7.31 (d, *J* = 8.2 Hz, 2H, ArH), 8.08 (d, *J* = 8.3 Hz, 2H, ArH), 8.56 (s, 1H, CH) ppm; **^{13}C NMR** (75 MHz, $CDCl_3$): δ δ 15.0, 28.4, 29.1, 29.2, 116.4, 128.0, 130.2, 134.5, 150.9, 151.4, 159.5, 160.6, 162.8 ppm; **HRMS** (APCI) m/z: Molecular formula: $C_{15}H_{16}N_2O_3$, Calcd for $[M+H]^+$ 273.1239; Found 273.1234; ppm error 0.27.

5-(4-Methoxybenzylidene)-1,3-dimethylpyrimidine-2,4,6(1*H*,3*H*,5*H*)-trione (3)

Yield = 75%; **State** = Solid; **Colour** = Lemon Yellow; **^{1}H NMR** (400 MHz, $CDCl_3$): δ 3.40 (s, 3H, CH_3), 3.42 (s, 3H, CH_3), 3.91 (s, 3H, OCH_3), 6.98 (d, *J* = 9.0 Hz, 2H, ArH), 8.33 (d, *J* = 8.8 Hz, 2H, ArH), 8.52 (s, 1H, CH) ppm; **^{13}C NMR** (100 MHz, $CDCl_3$): δ 28.4, 29.1, 55.6, 114.0, 114.3, 125.6, 138.0, 151.4, 158.9, 161.0, 163.2, 164.3 ppm; **HRMS** (APCI) m/z: Molecular formula: $C_{14}H_{14}N_2O_3$, Calcd for $[M+H]^+$ 275.1032; Found 275.1025; ppm error -0.33.

1,3-Diethyl-5-(4-methoxybenzylidene)-2-thioxodihydropyrimidine-4,6(1*H*,5*H*)-dione (4)

Yield = 42%; **State** = Solid; **Colour** = Dark Yellow; **^{1}H NMR** (500 MHz, $CDCl_3$): δ 1.32 (t, *J* = 6.9Hz, 6H, CH_3), 3.92 (s, 3H, OCH_3), 4.57 (q, *J* = 6.9 Hz, 4H, CH_2), 6.99 (d, *J* = 8.9 Hz, 2H, ArH), 8.35 (d, *J* = 8.9 Hz, 2H, ArH), 8.51 (s, 1H, CH) ppm; **^{13}C NMR** (125 MHz, $CDCl_3$): δ 12.4, 12.5, 43.6, 44.2, 55.7, 114.1, 115.1, 126.0, 138.3, 158.9, 160.1, 161.4, 164.7, 179.0 ppm; **HRMS** (APCI) m/z: Molecular formula: $C_{16}H_{18}N_2O_3S$, Calcd for $[M+H]^+$ 319.1116; Found 319.1115; ppm error 0.93

1,3-Diethyl-5-(4-hydroxy-3,5-dimethoxybenzylidene)-2-thioxodihydropyrimidine-4,6(1*H*,5*H*)-dione (5)

Yield = 83%; **State** = Solid; **Colour** = Yellowish Orange; **^{1}H NMR** (500 MHz, $CDCl_3$): δ 1.32 (t, *J* = 7.0 Hz, 6H, CH_3), 3.99 (s, 6H, OCH_3), 4.55-4.62 (m, 4H, CH_2), 6.33 (bs, 1H, OH), 7.88 (s, 2H, ArH), 8.45 (s, 1H, CH) ppm; **^{13}C NMR** (100 MHz, $CDCl_3$): δ 12.4, 12.5, 43.6, 44.2, 56.5, 113.5, 115.1, 124.6, 141.6, 146.5, 158.9, 160.5, 161.6, 178.9 ppm; **HRMS** (APCI) m/z Molecular formula: $C_{17}H_{20}N_2O_5S$, Calcd for $[M+H]^+$ 365.1171; Found 365.1171; ppm error 0.74.

1,3-Dimethyl-5-(2,4,5-trimethoxybenzylidene)pyrimidine-2,4,6(1*H*,3*H*,5*H*)-trione (6). Yield = 97%; **State** = Solid; **Colour** = Yellow; **^{1}H NMR** (300 MHz, $CDCl_3$): δ 3.38 (s, 3H, CH_3), 3.41 (s, 3H, CH_3), 3.92-3.95 (m, 6H, OCH_3), 3.99 (s, 3H, OCH_3), 6.45 (s, 1H, ArH), 8.51 (s, 1H, ArH), 9.07 (s, 1H, CH) ppm; **^{13}C NMR** (75 MHz, $CDCl_3$): δ 28.4, 28.9, 56.2, 56.4, 56.5, 94.9, 112.9, 113.9, 116.0, 142.2, 151.7, 152.8, 156.6, 158.9, 161.3, 163.6 ppm; **HRMS** (APCI) m/z: Molecular formula: $C_{16}H_{18}N_2O_6$, Calcd for $[M+H]^+$ 335.1243; Found 335.1240; ppm error 0.68.

1,3-Diethyl-2-thioxo-5-(2,4,5-trimethoxybenzylidene)dihydropyrimidine-4,6(1*H*,5*H*)-dione (7). Yield = 97%; **State** = Solid; **Colour** = Red; **^{1}H NMR** (400 MHz, $CDCl_3$): δ 1.31 (q, *J* = 6.8 Hz, 6H, CH_3), 3.92 (s, 3H, OCH_3), 3.95 (s, 3H, OCH_3), 4.01 (s, 3H, OCH_3), 4.58 (q, *J* = 7.0 Hz, 4H, CH_2), 6.45 (s, 1H, ArH), 8.46 (s, 1H, ArH), 9.07 (s, 1H, CH) ppm; **^{13}C NMR** (75 MHz, $CDCl_3$): δ 12.4, 12.5, 43.5, 44.1, 56.2, 56.3, 56.5, 94.8, 113.5, 114.5, 115.7, 142.3, 153.9, 157.2, 159.2, 159.3, 161.8, 179.1 ppm; **HRMS** (APCI) m/z: Molecular formula: $C_{18}H_{22}N_2O_5S$, Calcd for $[M+H]^+$ 379.1328; Found 379.1322; ppm error -0.36.

1,3-Dimethyl-5-(3,4,5-trimethoxybenzylidene)pyrimidine-2,4,6(1*H*,3*H*,5*H*)-trione (8). Yield = 99%; **State** = Solid; **Colour** = Yellow; **^{1}H NMR** (400 MHz, $CDCl_3$): δ 3.40 (s, 3H, CH_3), 3.43 (s, 3H, CH_3), 3.94 (s, 6H, OCH_3), 3.99

(s, 3H, OCH_3), 7.72 (s, 2H, ArH), 8.47 (s, 1H, CH) ppm; **^{13}C NMR** (100 MHz, $CDCl_3$): δ 28.5, 29.2, 56.3, 61.1, 106.7, 113.0, 115.8, 127.5, 143.4, 151.3, 152.4, 153.7, 159.0, 160.8, 163.0 ppm; **HRMS** (APCI) m/z: Molecular formula: $C_{16}H_{18}N_2O_6$, Calcd for $[M+H]^+$ 335.1243; Found 335.1238; ppm error 0.07.

5-(3-Ethoxy-4-hydroxybenzylidene)-1,3-diethyl-2-thioxodihydropyrimidine-4,6(1*H,*5*H*)-dione (9). Yield = 75%; **State** = Solid; **Colour** = Yellow; **^{1}H NMR** (400 MHz, $CDCl_3$): δ 1.31 (t, *J* = 6.9 Hz, 6H, CH_3), 1.51 (t, *J* = 7.0 Hz, 3H, CH_3), 4.24 (q, *J* = 7.0 Hz, 2H, CH_2), 4.53-4.61 (m, 4H, CH_2), 6.48 (bs, 1H, OH), 7.0 (d, *J* = 8.4 Hz, 1H, ArH), 7.73 (d, *J* = 8.4 Hz, 1H, ArH), 8.42 (d, *J* = 1.9 Hz, 1H, ArH), 8.46 (s, 1H, CH) ppm; **^{13}C NMR** (75 MHz, $CDCl_3$): δ 12.4, 12.5, 14.7, 43.6, 44.2, 64.8, 114.5, 114.6, 117.2, 125.9, 133.6, 145.3, 152.3, 159.0, 160.6, 161.6, 178.9 ppm; **HRMS** (APCI) m/z: Molecular formula: $C_{17}H_{20}N_2O_4S$, Calcd for $[M+H]^+$ 348.1144; Found 348.1212; ppm error -1.22.

5-(3,4-Dimethoxybenzylidene)-1,3-diethyl-2-thioxodihydropyrimidine-4,6(1*H*,5*H*)-dione (10). Yield = 86%; **State** = Solid; **Colour** = Yellow; **^{1}H NMR** (400 MHz, $CDCl_3$): δ 1.32 (t, *J* = 6.9 Hz, 6H, CH_3), 3.98 (s, 3H, OCH_3), 3.99 (s, 3H, OCH_3), 4.54-4.60 (m, 4H, CH_2), 6.96 (d, *J* = 8.6 Hz, 1H, ArH), 7.84 (d, *J* = 8.7Hz, 1H, ArH), 8.34 (d, *J* = 2.1 Hz, 1H, ArH), 8.48 (s, 1H, CH) ppm; **^{13}C NMR** (100 MHz, $CDCl_3$): δ 12.4, 12.5, 43.6, 44.2, 56.1, 56.2, 110.5, 115.1, 116.7, 126.2, 132.8, 148.5, 154.7, 158.9, 160.2, 161.5, 178.9 ppm; **HRMS** (APCI) m/z: Molecular formula: $C_{17}H_{20}N_2O_4S$, Calcd for $[M+H]^+$ 348.1144; Found 348.1213; ppm error -0.94.

(*E*)-1,3-Dimethyl-5-(3-phenylallylidene)pyrimidine-2,4,6(1*H*,3*H*,5*H*)-trione (11). Yield = 88%; **State** = Solid; **Colour** = Yellowish Orange; **^{1}H NMR** (400 MHz, $CDCl_3$): δ 3.38 (s, 6H, CH_3), 7.40-7.46 (m, 4H, ArH), 7.65-7.69 (m, 2H, CH), 8.21 (d, *J* = 12.0 Hz, 1H, ArH), 8.55-8.64 (m, 1H, CH); **^{13}C NMR** (100 MHz, $CDCl_3$): δ 28.1, 28.7, 114.5, 125.1, 129.1, 129.2, 131.5, 135.3, 151.5, 154.3, 157.4, 161.7, 162.3 ppm; **HRMS** (APCI) m/z: Molecular formula: $C_{15}H_{14}N_2O_3$, Calcd for $[M-H]^+$ 269.0926; Found 269.0941; ppm error 3.5.

(*E*)-1,3-Diethyl-5-(3-phenylallylidene)-2-thioxodihydropyrimidine-4,6(1*H*,5*H*)-dione (12). Yield = 54%; **State** = Solid; **Colour** = Yellow; **^{1}H NMR** (400MHz, $CDCl_3$): δ 1.31 (q, *J* = 7.3 Hz, 6H, CH_3), 4.50-4.60 (m, 4H, CH_2), 7.39-7.5 (m, 4H, ArH), 7.63-7.76 (m, 2H, CH), 8.23 (d, *J* = 12.1 Hz, 1H, ArH), 8.57-8.69 (m, 1H, CH); **^{13}C NMR** (100MHz, $CDCl_3$): δ 12.4, 12.5, 43.3, 43.8, 115.3, 125.7, 129.2, 129.3, 131.8, 135.3, 155.0, 158.6, 159.7, 160.5, 179.0 ppm; **HRMS** (APCI) m/z: Molecular formula: $C_{17}H_{18}N_2O_2S$, Calcd for $[M+H]^+$ 315.1167; Found 315.1161; ppm error 0.3.

(*E*)-5-(3-(2-Methoxyphenyl)allylidene)-1,3-dimethylpyrimidine-2,4,6(1*H*,3*H*,5*H*)-trione (13). Yield = 91%; **State** = Solid; **Colour** = Orange; **^{1}H NMR** (500 MHz, $CDCl_3$): δ 3.38 (d, *J* = 2.8 Hz, 6H, CH_3), 3.93 (s, 3H, OCH_3), 6.93 (d, *J* = 8.4 Hz, 1H, CH), 7.00 (t, *J* = 7.5 Hz, 1H, CH), 7.38-7.43 (m, 1H, ArH), 7.76 (d, *J* = 7.8 Hz, 1H, ArH), 7.87 (d, *J* = 15.5 Hz, 1H, ArH), 8.24 (d, *J* = 12.1 Hz, 1H, ArH), 8.57-8.64 (m, 1H, CH); **^{13}C NMR** (75 MHz, $CDCl_3$): δ 28.0, 28.7, 55.7, 111.3, 113.6, 121.0, 124.4, 125.2, 128.9, 133.2, 149.7, 151.6, 158.6, 158.9, 161.8, 162.5 ppm; **HRMS** (APCI) m/z: Molecular formula: $C_{16}H_{16}N_2O_4$, Calcd for $[M-H]^+$ 299.1032; Found 299.1046; ppm error 3.2.

(*E*)-1,3-Diethyl-5-(3-(2-methoxyphenyl)allylidene)-2-thioxodihydropyrimidine-4,6(1*H*,5*H*)-dione (14). Yield = 76%; **State** = Solid; **Colour** = Red; **^{1}H NMR** (500 MHz, $CDCl_3$): δ 1.28-1.34 (m, 6H, CH_3), 3.93 (s, 3H, OCH_3), 4.52-4.58 (m, 4H, CH_2), 6.93 (d, *J* = 8.3 Hz, 1H, CH), 7.00 (t, *J* = 7.5 Hz, 1H, CH), 7.40-7.45 (m, 1H, ArH), 7.80 (d, *J* = 7.8 Hz, 1H, ArH), 7.93 (d, *J* = 15.5 Hz, 1H, ArH), 8.26 (d, *J* = 12.2 Hz, 1H, ArH), 8.58-8.66 (m, 1H, CH) ppm; **^{13}C NMR** (75 MHz, $CDCl_3$): δ 12.4, 12.5, 43.2, 43.7, 55.8, 111.4, 114.4, 121.0, 124.4, 125.6, 128.9, 133.6, 150.5, 159.0, 159.8, 160.7, 179.0; **HRMS** (APCI) m/z: Molecular formula: $C_{18}H_{20}N_2O_3S$, Calcd for $[M+H]^+$ 344.1195; Found 344.1209; ppm error 2.7.

(*E*)-1,3-Dimethyl-5-(3-(2-nitrophenyl)allylidene)pyrimidine-2,4,6(1*H*,3*H*,5*H*)-trione (15). Yield = 97%; **State** = Solid; **Colour** = Lemon Yellow; **^{1}H NMR** (500 MHz, $CDCl_3$): δ 3.36-3.47 (m, 6H, CH_3), 7.54-7.63 (m, 1H, CH), 7.65-7.75 (m, 1H, CH), 7.87-7.98 (m, 2H, ArH), 8.02-8.12 (m, 1H, ArH), 8.18-8.30 (m, 1H, ArH), 8.47-8.64 (m, 1H, CH) ppm; **^{13}C NMR** (75 MHz, $CDCl_3$): δ 28.2, 28.9, 116.8, 125.2, 129.0, 129.4, 130.8, 131.0, 133.5, 147.0, 148.5, 151.3, 155.8, 161.5, 161.8 ppm; **HRMS** (APCI) m/z: Molecular formula: $C_{15}H_{13}N_3O_5$, Calcd for $[M+H]^+$ 316.0933; Found 316.0928; ppm error 0.2.

(*E*)-1,3-Diethyl-5-(3-(2-nitrophenyl)allylidene)-2-thioxodihydropyrimidine-4,6(1*H*,5*H*)-dione (16). Yield = 76%; **State** = Solid; **Colour** = Yellow; **^{1}H NMR** (300 MHz, $CDCl_3$): δ 1.27-1.34 (m, 6H, CH_3), 4.54 (q, *J* = 7.0 Hz, 4H, CH_2), 7.55-7.62 (m, 1H, CH), 7.69 (t, *J* = 7.6 Hz, 1H, CH), 7.90-7.99 (m, 2H, ArH), 8.06 (d, *J* = 8.1 Hz, 1H, ArH), 8.23 (d, *J* = 11.9 Hz, 1H, ArH), 8.50-8.62 (m, 1H, CH) ppm; **^{13}C NMR** (100 MHz, $CDCl_3$): δ 12.4, 12.5, 43.4, 43.9, 117.5, 125.2, 129.4, 129.5, 130.8, 131.1, 133.5, 147.4, 148.5, 156.8, 159.5, 160.0, 178.8 ppm; **HRMS** (APCI) m/z: Molecular formula: $C_{17}H_{17}N_3O_4S$, Calcd for $[M+H]^+$ 359.0940; Found 359.0953; ppm error 3.9.

(*E*)-5-(3-(4-Methoxyphenyl)allylidene)-1,3-dimethylpyrimidine-2,4,6(1*H*,3*H*,5*H*)-trione (17). Yield = 86%; **State** = Solid; **Colour** = Yellow; **^{1}H NMR** (500 MHz, $CDCl_3$): δ 3.37 (s, 6H, CH_3), 3.87 (s, 3H, OCH_3), 6.93 (d, *J* = 8.8 Hz, 2H, ArH), 7.39 (d, *J* = 15.3 Hz, 1H, CH), 7.63 (d, *J* = 8.8 Hz, 2H, ArH), 8.18 (d, *J* = 12.2 Hz, 1H, CH), 8.44-8.51 (m, 1H, CH) ppm; **^{13}C NMR** (100 MHz, $CDCl_3$): δ 28.0, 28.6, 55.5, 113.0, 114.7, 123.1, 128.3, 131.3, 151.6, 154.8, 158.0, 162.0, 162.5, 162.8 ppm; **HRMS** (APCI) m/z: Molecular formula: $C_{16}H_{16}N_2O_4$, Calcd for $[M+H]^+$ 301.1188; Found 301.1186; ppm error 1.0.

(*E*)-1,3-Diethyl-5-(3-(4-methoxyphenyl)allylidene)-2-thioxodihydropyrimidine-4,6(1*H*,5*H*)-dione (18). Yield = 87%; **State** = Solid; **Colour** = Red; **^{1}H NMR** (400 MHz, $CDCl_3$): δ 1.31 (q, *J* = 8.3 Hz, 6H, CH_3), 3.88 (s, 3H, OCH_3), 4.50-4.59 (m, 4H, CH_2), 6.94 (d, *J* = 8.8 Hz, 2H, ArH), 7.44 (d, *J* = 15.2 Hz, 1H, CH), 7.67 (d, *J* = 8.8 Hz, 2H, ArH), 8.21 (d, *J* = 12.2 Hz, 1H, CH), 8.47-8.56 (m, 1H, CH); **^{13}C NMR** (100 MHz, $CDCl_3$): δ 12.4, 12.5, 43.2, 43.7, 55.6, 113.8, 114.8, 123.7, 128.3, 131.6, 155.7, 159.2, 160.0, 160.8, 163.0, 179.0 ppm; **HRMS** (APCI) m/z: Molecular formula: $C_{18}H_{20}N_2O_3S$, Calcd for $[M+H]^+$ 344.1195; Found 344.1210; ppm error 3.1.

(*E*)-1,3-Dimethyl-5-(3-(4-nitrophenyl)allylidene)pyrimidine-2,4,6(1*H*,3*H*,5*H*)-trione (19). Yield = 89%; **State** = Solid; **Colour** = Yellow; **^{1}H NMR** (400 MHz, $CDCl_3$): δ 3.40 (s, 6H, CH_3), 7.42 (d, *J* = 15.6 Hz, 1H, CH), 7.80 (d, *J* = 8.7 Hz, 2H, ArH), 8.19 (d, *J* = 11.8 Hz, 1H, CH), 8.27 (d, *J* = 8.8 Hz, 2H, ArH), 8.66-8.75 (m, 1H, CH) ppm; **HRMS** (APCI) m/z: Molecular formula: $C_{15}H_{13}N_3O_5$, Calcd for $[M+H]^+$ 315.0855; Found 315.0865; ppm error 1.4.

(E)-1,3-Diethyl-5-(3-(4-nitrophenyl)allylidene)-2-thioxodihydropyrimidine-4,6(1*H*,5*H*)-dione (20). Yield = 71%; **State** = Solid; **Colour** = Brick Red; **^{1}H NMR** (400 MHz, $CDCl_3$): δ 1.31 (q, *J* = 7.1 Hz, 6H, CH_3), 4.51-4.58 (m, 4H, CH_2), 7.45 (d, *J* = 15.5 Hz, 1H, CH), 7.83 (d, *J* = 8.7 Hz, 2H, ArH), 8.19 (d, *J* = 11.9 Hz, 1H, CH), 8.28 (d, *J* = 8.8 Hz, 2H, ArH), 8.67-8.76 (m, 1H, CH) ppm; **^{13}C NMR** (100 MHz, $CDCl_3$): δ 12.4, 12.5, 43.4, 43.9, 117.5, 124.3, 129.1, 129.4, 141.1, 148.8, 149.7, 156.2, 159.4, 160.1, 178.7 ppm; **HRMS** (APCI) m/z: Molecular formula: $C_{17}H_{17}N_3O_4S$, Calcd for $[M+H]^+$ 360.1018; Found 360.1012; ppm error -0.07.

Crystal Structure

Compounds **1**, **2** and **8** were obtained as single crystals by slow evaporation method and were solved using single - XRD (CCDC deposition no 2351679, 2391313 and 2440178). **Table 1** shows the experimental details of **1**, **2** and **8**.

X-ray data for the compound was collected at room temperature on a Bruker D8 QUEST instrument with an IμS Mo microsource (λ = 0.7107 A) and a PHOTON-III detector. The raw data frames were reduced and corrected for absorption effects using the Bruker Apex 3 software suite programs.[15] The structure was

solved using intrinsic phasing method and further refined with the SHELXL program and expanded using Fourier techniques.[16] Anisotropic displacement parameters were included for all non-hydrogen atoms. All C bound H atoms were positioned geometrically and treated as riding on their parent C atoms [C-H = 0.93-0.97 Å, and Uiso(H) = 1.5Ueq(C) for methyl H or 1.2Ueq(C) for other H atoms].

Table 1. Experimental details of the crystals **1**, **2** and **8**.

Identification code	**1**	**2**	**8**
Empirical formula	$C_{13}H_{11}BrN_2O_3$	$C_{15}H_{16}N_2O_3$	$C_{16}H_{18}N_2O_6$
Formula weight	323.147	272.30	334.32
Temperature/K	294.15	294(2)	294(2)
Crystal system	triclinic	monoclinic	triclinic
Space group	P-1	$P2_1$	P-1
a/Å	7.9285(3)	9.1839(9)	9.5938(4)
b/Å	8.0210(4)	5.9593(6)	12.5580(6)
c/Å	11.7158(6)	12.8027(13)	14.3048(7)
α/°	88.7261(16)	90	105.6969(16)
β/°	74.8280(14)	101.613(3)	101.3802(17)
γ/°	63.1085(13)	90	98.8776(15)
Volume/Å^3	637.32(5)	686.34(12)	1586.65(13)
Z	2	2	4
ρ_{calc}g/cm^3	1.684	1.318	1.400
μ/mm^{-1}	3.230	0.093	0.108
F(000)	323.8	288.0	704.0
Crystal size/mm^3	0.2 × 0.18 × 0.16	0.22 × 0.18 × 0.16	0.22 × 0.18 × 0.16
Radiation	Mo Kα (λ = 0.71073)	MoKα (λ = 0.71073)	MoKα (λ = 0.71073)
2Θ range for data collection/°	5.74 to 56.74	6.498 to 56.79	3.056 to 56.646
Index ranges	-10 ≤ h ≤ 10, -10 ≤ k ≤ 10, -15 ≤ l ≤ 15	-12 ≤ h ≤ 12, -7 ≤ k ≤ 7, -17 ≤ l ≤ 17	-12 ≤ h ≤ 12, -16 ≤ k ≤ 16, -19 ≤ l ≤ 19
Reflections collected	15972	17905	36254
Independent reflections	3170 [R_{int} = 0.0558, R_{sigma} = 0.0423]	3400 [R_{int} = 0.0679, R_{sigma} = 0.0569]	7874 [R_{int} = 0.0429, R_{sigma} = 0.0390]
Data/restraints/parameters	3170/0/175	3400/1/184	7874/0/443
Goodness-of-fit on F^2	1.110	1.037	1.052
Final R indexes [I>=2σ (I)]	R_1 = 0.0319, wR_2 = 0.0816	R_1 = 0.0473, wR_2 = 0.1126	R_1 = 0.0497, wR_2 = 0.1358
Final R indexes [all data]	R_1 = 0.0697, wR_2 = 0.0937	R_1 = 0.0848, wR_2 = 0.1335	R_1 = 0.0859, wR_2 = 0.1584
Largest diff. peak/hole / e Å^{-3}	1.71/-1.28	0.18/-0.22	0.21/-0.16

Flack parameter	-0.7(7)

Biology

MIC assay

Using the broth microdilution method according to CLSI (formerly known as NCLS) guidelines, peptides or synthesized test molecules (**1-10**) were tested for their *in vitro* antibacterial activity, against gram-negative bacteria [*Acinetobacter baumannii* ATCC (1605), *Klebsiella pneumoniae* ATCC (27736), *Escherichia coli* ATCC (25922), *Pseudomonas aeruginosa* ATCC (27853)], and gram-positive bacteria [*Staphylococcus aureus* ATCC (25923)] using microtiter broth dilution method, as prescribed by CLSI and as described by Pasupuleti et al. (2009) and Horam et al. (2019).[17] Briefly, bacteria were grown overnight in 3% TSB to the mid-logarithmic phase, centrifuged, and washed twice in 10 mM Tris, pH 7.4, then re-suspended in 2X cation-adjusted MHB broth (Becton Dickinson, USA) to achieve a concentration of 1×10^5 CFU/mL. In a 96-well microtiter plate (polypropylene, Costar Corp., Cat. No. 3790), serially diluted compounds (**1-10**) at concentrations (160 µM to 0.31 µM) were added to each well, followed by the addition of 50 µL of 2X cation-adjusted MHB broth containing 1×10^5 CFU/mL bacteria. The plate was incubated at 37 °C for 16 hours. MIC values were determined by visual inspection of the plates, with values considered where growth inhibition exceeded 90%. To rule out biasness and human error, 20 µL of 0.01% resazurin dye was added and incubated for 30 min. The development of pink color indicated the growth of microbes, while blue color indicated inhibition of the bacterial growth. The data was correlated to the visual observation. MIC was taken as the concentration at the lowest concentration where we observed the blue color. All the MIC determination assay were performed in triplicate. A negative control, where no peptide was added, was included in each assay, while LL37 peptide was used as a positive control.

Cytotoxicity assay

Cell viability studies of the potent synthesized test molecules (**1-20**) were carried out against MCF-7 using MTT assays. Briefly, Vero cells (3000 cells/well) were seeded in 96-well plates and grown in DMEM medium supplemented with 10% FBS and 1 X antimycotic and antibacterial solution (Sigma, USA) at 37 °C and 5% CO_2 to confluence. After the incubation, test compounds to be investigated were diluted (i.e., 12.5, 25, 50 and 100 µg/mL) in DMEM medium and added to the cells along with appropriate controls. After 24 hours of incubation, the supernatant was discarded, and fresh media was added to the cells along with 200 µL of the MTT solution (0.5 mg in RPMI 1640 medium). After 1 hour of incubation at 37 °C in 5 % CO_2, the media was discarded, and DMSO was added to it. The plate was incubated at room temperature for 30 mins under gently shaking conditions. Later, the dissolved blue formazan was transferred to fresh 96 plates and the absorbance was monitored at 570 nm. The results represent here the pooled mean values obtained from independent triplicate measurements

Acknowledgements

The authors thank the Director CSIR-IICT, for providing the required facilities (IICT/Pubs./2026/022). AS thank DST for INSPIRE Faculty grant (GAP1039). The authors acknowledge the use of the X-ray crystallography facility at CSIR-IICT and thank Dr B Sridhar for supervising data collection, structure solution, and refinement.

Supplementary Material

The characterization data is provided as Supplementary Information

References

1. Savoia, D., *Curr. Drug Targets*, **2016**. *17*, 731–738.
2. Sommer, M.O.A., C. Munck, R.V. Toft-Kehler, and D.I. Andersson, *Nat. Rev. Microbiol.*, **2017**. *15*, 689–696.
3. Southey, M.W.Y. and M. Brunavs, *Front. Drug Discov.*, **2023**. *Volume 3 - 2023*.
4. Scott, D.E., A.R. Bayly, C. Abell, and J. Skidmore, *Nat. Rev. Drug Discov.*, **2016**. *15*, 533–550.
5. Kaur, N., M. Kaur, H.S. Sohal, H. Han, and P.K. Bhowmik *A Review on Barbituric Acid and Its Derivatives: Synthesis, Reactions, and Bio-Applications*. Organics, 2024. **5**, 298–345 DOI: 10.3390/org5030017.
6. Laxmi, S.V., G. Rajitha, B. Rajitha, and A.J. Rao, *J. Chem. Biol.*, **2016**. *9*, 57–63.
7. Liu, H., Y. Liu, C. Yuan, G.-P. Wang, S.-F. Zhu, Y. Wu, B. Wang, Z. Sun, Y. Xiao, Q.-L. Zhou, and H. Guo, *Org. Lett.*, **2016**. *18*, 1302–1305.
8. Lee, S.Y., B. Slagle-Webb, A.K. Sharma, and J.R. Connor, *Anticancer Res.*, **2020**. *40*, 6039.
9. Liao, Y.-J., S.-M. Hsu, C.-Y. Chien, Y.-H. Wang, M.-H. Hsu, and F.-M. Suk, *Molecules*, **2020**. *25*, 2856.
10. Ghadami, S.A., L. Hosseinzadeh, E. Eskandari, N. Yarmohammadi, and H. Adibi, *Mol. Biol. Rep.*, **2021**. *48*, 7637–7646.
11. Sharma, A., S. Noki, S.J. Zamisa, H.A. Hazzah, Z.M. Almarhoon, A. El-Faham, B.G. de la Torre, and F. Albericio, *ChemMedChem*, **2018**. *13*, 1923–1930.
12. Al Rasheed, H., K. Dahlous, A. Sharma, E. Sholkamy, A. El-Faham, B.G. de la Torre, and F. Albericio, *ACS Omega*, **2020**. *5*, 15805–15811.
13. Sharma, A., S.J. Zamisa, S. Noki, Z. Almarhoon, A. El-Faham, B.G.d.l. Torre, and F. Albericio, *Acta Crystallogr. Sect. C Struct. Chem.*, **2018**. *74*, 1703–1714.
14. Kaur, P. and R. Sharma, *Biochem. Biophys. Res. Commun.*, **2025**. *785*, 152709.
15. Bruker, S. and S. SAINT, *Bruker AXS Inc*, in *Madison, Wisconsin, USA*. 2016.
16. Sheldrick, G., *Acta Crystallographica Section C*, **2015**. *71*, 3–8.
17. Strömstedt Adam, A., M. Pasupuleti, A. Schmidtchen, and M. Malmsten, *Antimicrobial Agents and Chemotherapy*, **2009**. *53*, 593–602.

